Materials Advances

ROYAL SOCIETY OF CHEMISTRY

COMMUNICATION

View Article Online
View Journal | View Issue

Cite this: *Mater. Adv.*, 2022, 3, 937

Received 26th September 2021,
Accepted 28th November 2021

DOI: 10.1039/d1ma00887k

rsc.li/materials-advances

Environmentally friendly carrageenan-based ionic-liquid driven soft actuators†

João P. Serra,[a] Liliana C. Fernandes,[ab] Daniela M. Correia,*[ac] Carmen R. Tubio,[b] José L. Vilas-Vilela,[bd] Mohammad Tariq,[e] José M. S. S. Esperança,[e] Carlos M. Costa[af] and Senentxu Lanceros-Mendez*[bg]

A naturally derived polymer based on iota carrageenan and different ammonium and imidazolium based ionic liquids (ILs) are used for the development of environmentally friendly soft actuators. The influence of IL content and type and solvent evaporation temperature on the morphological and physico-chemical properties of the materials was evaluated, together with the effect on actuator functional response. Independently of the IL content and type, and the solvent evaporation temperature, a non-porous structure is obtained. The incorporation of the IL within the polymer matrix does not affect the thermal stability but leads to a decrease in the Young modulus for the different IL/carrageenan samples. The highest influence was observed by using the [Ch][DHP] IL at a filler content of 40% w/w with a decrease in the Young modulus from 748 MPa for the neat polymer to 145 MPa for the [Ch][DHP]/carrageenan sample. Furthermore, the ionic conductivity of the samples increases with increasing IL content, with the highest values being 2.9 × 10^{-6} S cm^{-1} and 1.2 × 10^{-6} S cm^{-1} for the samples with 40% w/w of [Bmim][$FeCl_4$] and [Ch][DHP], respectively. Regarding the soft actuator performance, the maximum displacement was obtained for the [Ch][DHP]/carrageenan sample with an IL content of 40% w/w, showing a maximum displacement of 5.8 mm at a DC applied voltage of 9 V.

Introduction

Smart materials possess the ability to change their properties in a controlled manner in response to external stimuli.[1] These stimuli are associated with variations in environmental conditions (*e.g.* temperature, pressure, or light) or specific stimuli such as pH variations, enzymatic action, and magnetic, electrical or mechanical solicitations.[2,3] Due to their versatility, they can be applied in a large variety of areas including tissue engineering,[4] photocatalytic applications[5] or energy storage.[6] One of the most important implementation areas, nevertheless, is in sensor and actuator applications.[7,8]

In particular, smart materials are able to convert an electrical stimulus into a mechanical response, leading therefore to suitable actuator responses.[9] Polymer-based actuators, typically identified as soft actuators, have gained increasing attention in areas including biomedicine, packaging, factory automation, microelectronics, or robotics, among others.[10] To improve actuator performance or even to add further functionalities, fillers such as ionic liquids (ILs) are being explored.[11] ILs are defined as liquid salts at convenient working temperatures (conventionally below 100 °C), composed solely of anions and cations, with a large potential to be applied in the design of actuators due to their high electrochemical window and ionic conductivity, among others, that can be tuned by designing specific cation/anion combinations.[12] ILs also present other relevant physico-chemical characteristics such as almost non-volatility and non-flammability, air and water stability, as well as good dispersion and null agglomeration in solutions.[11,13]

Most IL/polymer based actuators are composed by synthetic polymers derived from fossil fuels, such as poly(vinylidene fluoride) (PVDF) and its copolymers,[14] poly(ethylene oxide)

[a] *Centre of Physics, University of Minho, Braga 4710-053, Portugal. E-mail: d.correia@fisica.uminho.pt*
[b] *BCMaterials, Basque Center for Materials, Applications and Nanostructures, UPV/EHU Science Park, Leioa 48940, Spain. E-mail: senentxu.lanceros@bcmaterials.net*
[c] *Centre of Chemistry, University of Trás-os-Montes e Alto Douro, Vila Real, 5000-801, Portugal*
[d] *Departamento de Química Física, Facultad de Ciencia y Tecnología, Universidad del País Vasco (UPV/EHU), Apdo. 644, Bilbao, Spain*
[e] *LAQV, REQUIMTE, Departamento de Química, Faculdade de Ciências e Tecnologia, Universidade NOVA de Lisboa, Caparica, 2829-516, Portugal*
[f] *Institute of Science and Innovation for Bio-Sustainability (IB-S), University of Minho, Braga 4710-053, Portugal*
[g] *Ikerbasque, Basque Foundation for Science, Bilbao 48009, Spain*

† Electronic supplementary information (ESI) available: Fig. S1 shows the Nyquist plots at 30 and 60 °C for the IL/carrageenan samples comprising 40% wt of the different ILs obtained at a solvent evaporation temperature of 80 °C. Video S1 shows the maximum displacement developed by the sample [Ch][DHP]/carrageenan comprising 40% w/w of IL. See DOI: 10.1039/d1ma00887k

(PEO),[15] and poly(L-lactic acid) (PLA),[16] among others,[17–19] mainly based on their mechanical, thermal, and chemical stability. However, industry and society demand a new generation of materials in the scope of sustainable and circular economy paradigms.[20] In fact, environmental problems such as global warming related issues, may be aggravated in the next few decades and several of those problems are caused by a lifestyle strongly dependent on fossil fuels.[21] In this scope, a reduction of the dependence on fossil fuel derived products is necessary.[22] In this sense, the replacement of synthetic polymers by natural and biopolymers is an urgent need.

Natural polymers are a class of materials produced by biological and renewable resources (plants and animals), many of them being biodegradable and/or biocompatible, allowing also to improve reuse and recyclability.[23] Natural materials can be classified into six different groups: lignin, polyesters, polyisoprenes, polynucleotides, polysaccharides and proteins, giving rise to different types of natural polymers, such as agar, alginates, cardlan, carrageenan, cellulose, chitin, galactomannans, gelatin, hyaluronan, pectin or xanthan, which can be selected for applications based on their different physico-chemical, thermal and mechanical properties.[24]

Carrageenans are sulphated polysaccharides extracted from red marine algae and they allow the formation of stiff and thermoreversible gels at room temperature.[25] Carrageenans are linear polymers composed of 1,3-linked β-D-galactose and 1,4-linked α-D-galactose.[26,27] All carrageenans show high molecular flexibility and in high concentrations they can form a double-helical structure.[28] There are different types of carrageenan which are designated by the Greek alphabet letters (kappa (κ-), iota (ι-), lambda (λ-), nu (ν-), mu (μ-) and theta (θ-)).[29] The most used are the first three and they differ in the number of sulphate groups and in the content of 3,6-anhydro-galactose. Thus, κ-carrageenan has one, ι-carrageenan has 2 and λ-carrageenan has 3 of these sulphate groups.[30,31] I-Carrageenan is one of the natural polymers with a large abundance in nature, biodegradability and low cost.[32,33] This type of carrageenan is considered a promising and environmentally friendly material for electronic devices but has a low ionic conductivity when compared with other types of carrageenan.[34] Recently, the potential of carrageenan hydrogels as actuators has been demonstrated,[43] with the use of different types of carrageenan (κ, ι and λ) combined with poly(3-hexylthiophene) (P3HT) allowing the tailoring of the electrical and electrochemical properties of neat carrageenan hydrogels.[43] However, besides the great interest on soft actuators, natural polymers and ILs, the area of natural polymer based soft actuators is an emergent one, with a lack of studies concerning the suitable combination of natural polymers and ILs, despite its great potential in tuning material properties and functional performance.[11,35] Imidazolium-based ILs and epoxidized natural rubber (ENR), able to improve the polymer heat resistance and electrical conductivity have shown potential in applications as elastomeric sensors and actuators.[36] In another work, Migliorini *et al.*[37] combined the bioplastic poly(3-hydroxybutyrate) (PHB) with the ionic liquid 1-butyl-3-methylimidazolium bis(trifluoromethylsulfonyl)imide ([Bmim][TFSI]) producing soft actuators with a working window from 0.1 to 7 V and a displacement ranging from 0.2 to 17 mm, respectively.[37] Other natural polymers, such as cellulose incorporating hydroxyethyltrimethylammonium dihydrogen phosphate [Ch][DHP], have also been developed for actuator applications, displaying a displacement of 9 mm at 8 Vpp.[38]

Related to the use of carrageenan, electromechanical actuators have been developed based on poly(3-hexylthiophene)/carrageenan conductive hydrogels, the ι-hydrogel showing a deflection distance of 12.70 ± 0.1 mm and a deflection angle of 77.62 ± 0.35 at an electric field strength of 600 V mm^{-1}.[39] Thus, it seems interesting to further explore the potential of carrageenan as an actuator material, by the development of blends with ILs to tune electrical conductivity and mechanical properties, and therefore the functional response.

In the present work IL/carrageenan hybrid materials have been developed containing different ILs and produced at different solvent evaporation temperatures (25 and 80 °C). The ILs were selected attending to their high miscibility with water and taking into consideration the main focus of the study, related to the evaluation of the effect of IL cation and anion type on the IL–polymer matrix interaction and, as a consequence, on the actuator response. The effect of both IL type and content and solvent evaporation temperature on the morphological and physico-chemical properties of the materials was evaluated, together with the functional electromechanical actuator response. This study represents a contribution to the development of natural polymer based soft actuators, with strong potential for soft robotics and biomedical applications, among others.

Experimental section

Materials

Carrageenan (iota-ι type) (Fig. 1) was purchased from Alfa Aesar (Kandel, Germany) (Molecular weight 946.75 g mol^{-1}, impurity content of heavy metals <20 ppm). The ILs *N*-2-hydroxyethyl-*N*,*N*,*N*-trimethylammonium dihydrogen phosphate $>98\%$ [Ch][DHP], 1-butyl-3-methylimidazolium tetrachloroferrate(III) $>97\%$ [Bmim][$FeCl_4$], and 1-butyl-3-methylimidazolium tricyanomethanide 98% [Bmim][$C(CN)_3$] were supplied by Iolitec (Heilbronn, Germany). [Ch][$FeCl_4$] was prepared by the recipe used by Zhong *et al.*[40] with the change of the initial IL from [Bmim][Cl] to [Ch]Cl. The purity of the initial components ([Ch]Cl and $FeCl_3$) was higher than 99%, so the purity of

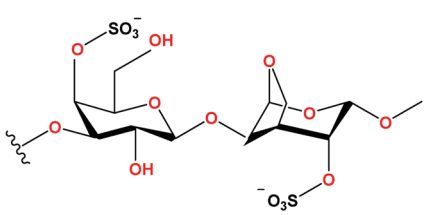

Fig. 1 Chemical structure of i-carrageenan.

Table 1 Chemical structure and relevant properties of the different ILs used in this work. (Data obtained from Iolitec)

IL	Structure		Molecular weight (g mol^{-1})	Density (ρ) (g m^{-3})	Conductivity (σ) (ms cm^{-1})
[Ch][DHP]	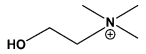	$H_2PO_4^{\ominus}$	201.16	—	<0.4
[Ch][$FeCl_4$]	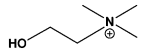	$FeCl_4^{\ominus}$	301.83	—	—
[Bmim][$FeCl_4$]	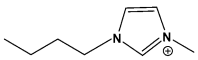	$FeCl_4^{\ominus}$	366.87	1.37	4.37
[Bmim][$C(CN)_3$]	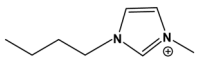	$C(CN)_3^{\ominus}$	229.28	1.05	8.83

[Ch][$FeCl_4$] is >99%. The chemical structure and relevant properties of the selected ILs are presented in Table 1.

Preparation of the neat and IL/carrageenan films

Neat carrageenan thin films were obtained by solvent casting after the dissolution of the polymer in ultrapure water (3/97% w/w) under magnetic stirring. For IL/carrageen composites, different amounts of [Ch][DHP] (10, 20 and 40% w/w) were first dispersed in ultrapure water for 10 minutes. Subsequently, carrageenan was added to the solution (3/97% w/w) and magnetically stirred at 40 °C. After complete polymer dissolution, the solution was spread on Petri dishes followed by solvent evaporation at different drying temperatures: 25 °C (3 days) and 80 °C (4 hours) in an oven (P-Selecta) (Barcelona, Spain) (Fig. 2). The thickness of the films is shown in Table 2.

To study the effect of IL type on the characteristics and actuator performance of these materials, different ILs ([Bmim][$FeCl_4$], [Bmim][$C(CN)_3$] and [Ch][$FeCl_4$]) were used at a 40% w/w concentration. In order to evaluate the effect of cation and anion on the hybrid material's physical–chemical characteristics, two ILs have been selected with different cations but a common anion, while the other two share a common cation but with different anions. IL/carrageen films based on these ILs were prepared following the solvent evaporation temperature of 80 °C.

Characterization of the thin films

After sputter coating the samples with a thin (200 nm) gold layer (Polaron, model SC502) (Göttingen, Germany), the morphology of the samples was evaluated by scanning electron microscopy (SEM, Zeiss EVO 40) (Göttingen, Germany) with an accelerating voltage of 20 kV. Energy-dispersive X-ray (EDX) analysis was carried out in a Hitachi Tabletop Microscope TM 3000 (Tokyo, Japan).

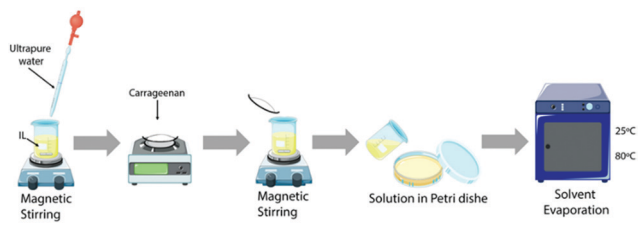

Fig. 2 Schematic representation of the procedure used for the preparation of the IL/carrageenan hybrid materials.

Table 2 Thickness of the IL/carrageenan films

IL/carrageenan	% w/w IL	Solvent evaporation temperature (°C)	Thickness ± 1 μm
[Ch][DHP]	0	25	85
	10		105
	20		92
	40		165
	40	80	119
[Ch][$FeCl_4$]	40		182
[Bmim][$FeCl_4$]	40		215
[Bmim][$C(CN)_3$]	40		247

The characteristic vibrational bands of the samples were evaluated at room temperature by Fourier transformed infrared (FTIR) spectroscopy in the Attenuated total reflection (ATR) mode using a Jasco FT/IR-6100 (Easton, USA). The spectra, in the 4000 to 600 cm^{-1} range were collected with 64 scans and a resolution of 4 cm^{-1}.

Differential scanning calorimetry (DSC) measurements were carried out in a PerkinElmer DSC 6000 (Massachusetts, EUA) in the temperature range between 25 °C and 200 °C at 10 °C min^{-1} under a nitrogen atmosphere.

Thermogravimetric (TGA) analysis was carried out in a PerkinElmer Pyris-1 TGA (Massachusetts, EUA) apparatus between 25 °C and 800 °C, at 10 °C min^{-1} under a nitrogen atmosphere.

Mechanical stress–strain measurements were performed in the tensile mode with a TST350 Linkam Instrument (Tadworth, England) set up at a strain rate of 15 μm s^{-1}.

Ionic conductivity and electromechanical characterization

The ionic conductivity of the different IL/carrageenan samples was measured by impedance analysis (real and imaginary impedance) in an Autolab PGSTAT-12 (Eco Chemie) (Utrecht, Netherlands) at frequencies between 500 mHz and 65 kHz and a temperature range from 25 to 70 °C, using a constant volume support equipped with gold blocking electrodes placed within a Buchi TO 50 oven (Flawil, Switzerland). The sample temperature was evaluated by means of a type K thermocouple placed close to the IL/carrageenan composites.

The ionic conductivity (σ) was determined by:

$$\sigma = \frac{t}{A \times R_b} \quad (1)$$

where t is the thickness, A is the area and R_b is the sample bulk resistivity, obtained by interception of the imaginary impedance (minimum value of Z'') with the slanted line in the real impedance (Z').

The electromechanical response of the IL/carrageenan films was evaluated by bending measurements using a PC connected to a Logitech HD 1080p Webcam camera (Lausanne, Switzerland). In the actuator design, two gold electrodes were deposited by magnetron sputtering, on both sides of the samples (dimensions of 2 mm × 12 mm), using a Polaron SC502 equipment (Göttingen, Germany). For the displacement measurements, the actuators were clamped with two needles and connected to an Agilent 33220A function generator (California, USA). The performance of the samples as actuators was evaluated in DC mode for applied voltages ranging from 4 V to 9 V.

Results and discussion

Morphological features

The morphology of neat carrageenan and the IL/carrageenan films was evaluated by SEM. The influence of IL content, type and solvent evaporation temperature were evaluated. Fig. 3a shows that neat carrageenan films present a non-porous structure with a cratered morphology as a result of its semicrystalline structure.[41] The incorporation of [Ch][DHP] leads to a more homogeneous cross-section surface, with irregularities in the films surface attributed to IL aggregation during the drying process. It is also important to notice that increasing the IL content up to 40% w/w led to a more compact structure, indicating that, independently of the [Ch][DHP] concentration, the IL is embedded into the carrageenan matrix.

The effect of the IL type and solvent evaporation temperature (25 °C and 80 °C) were also assessed. Similarly, as for the [Ch][DHP]/carrageenan samples, the incorporation of the [Bmim][$FeCl_4$] (Fig. 3d) induces a compact internal structure, when compared to neat carrageenan. Similar results are also observed upon the incorporation of 40% w/w of [Ch][$FeCl_4$] and [Bmim][$C(CN)_3$]. It is important to notice that for all samples, no significant differences are observed in their morphology when subjected to the different drying temperatures. Thus, we have mostly concentrated on the samples prepared at 80 °C based on the faster preparation.

The presence of ILs in the carrageen matrix was also assessed by EDX analysis. Fig. 4 shows the EDX cross section images for the different IL/carrageenan samples, comprising 40% w/w of each IL type obtained at a solvent evaporation temperature of 80 °C. For the sample containing [Ch][DHP] the phosphor (P) chemical element is identified through a yellow colour (Fig. 4a). Similarly, for [Ch][$FeCl_4$], [Bmim][$FeCl_4$] and [Bmim][$C(CN)_3$], iron (Fe) and nitrogen (N) are identified, respectively. It is confirmed that, independently of the IL type, all the EDX images shows a uniform IL distribution along the carrageenan matrix. Similar results were observed for the [Ch][DHP]/carrageenan samples comprising different IL contents obtained at 25 °C. It is also important to notice the presence of the element P in the surface of the [Ch][DHP]/carrageenan sample (Fig. 4a), indicating that some IL remains at the surface of the material.

Infrared vibrational bands and mechanical proprieties

The influence of the incorporation of different ILs on the chemical properties of the carrageenan matrix has been studied by FTIR-ATR measurements (Fig. 5a and b). Additionally, the effect of solvent evaporation temperature during the sample's preparation was also evaluated.

Fig. 5a shows the FTIR spectra of [Ch][DHP]/carrageenan samples with different IL contents obtained at different solvent drying temperatures. Independently of IL content and solvent evaporation temperature, the main carrageenan absorption bands are observed in the FTIR spectra. The absorption bands at 805, 845 and 905 cm^{-1} are attributed to the C–O–SO_3 bonds

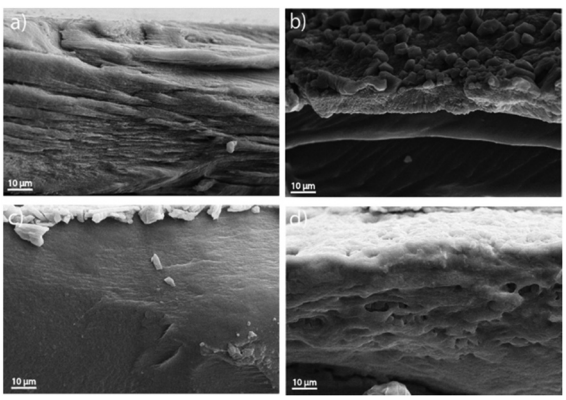

Fig. 3 Cross-section images of the IL/carrageenan composites with different IL contents obtained at different solvent evaporation temperatures: (a) 0% w/w at 25 °C, (b) 20% w/w of [Ch][DHP] at room temperature, (c) 40% w/w of [Ch][DHP] at 80 °C and (d) 40% w/w of [Bmim][$FeCl_4$] at 80 °C.

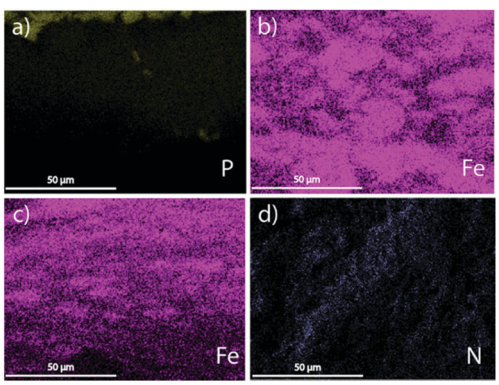

Fig. 4 EDS cross section images for the IL/carrageenan samples containing different ILs: (a) 40% w/w of [Ch][DHP], (b) 40% w/w of [Ch][$FeCl_4$], (c) 40% w/w of [Bmim][$FeCl_4$] and (d) 40% w/w of [Bmim][$C(CN)_3$]. All the samples were obtained at a solvent evaporation temperature of 80 °C.

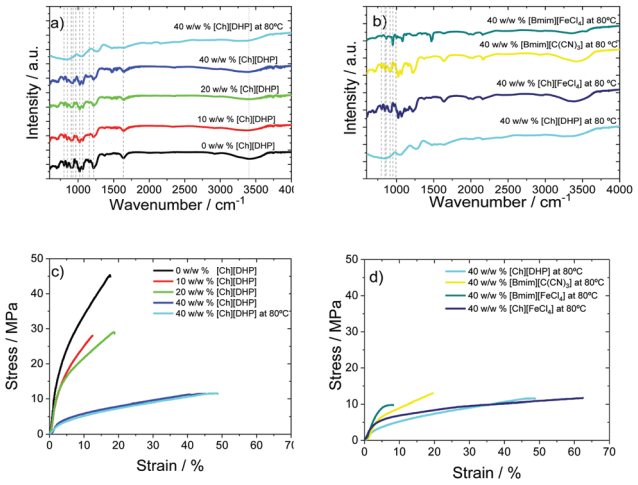

Fig. 5 (a and b) FTIR-ATR spectra and (c and d) stress–strain curves for: [Ch][DHP]/carrageenan samples containing different IL contents (10, 20 and 40% w/w) obtained at different drying temperatures (25 and 80 °C) and for IL/carrageenan samples comprising different ILs obtained at a solvent evaporation temperature of 80 °C, respectively.

at C2 of 3,6-anyhydrogalactose and to C4 and C6 of the galactose unit, respectively. The absorption bands that appear at 930 and 1070 cm^{-1} are attributed to the C–O bond of 3,6-anhydroglactose. The galactose groups are also identified at 970–975 cm^{-1} and the band appearing between 1240 and 1260 cm^{-1} is ascribed to an S=O bond of sulphate esters.[42] The band at 1635 cm^{-1} corresponds to the C=O asymmetric stretch/N–H deformation and at 3400 cm^{-1} to the OH/NH stretching.[43] The absorption bands of the IL [Ch][DHP] are observed at 1479 and 1644 cm^{-1}, corresponding to the CH_3 vibration and the band at 1644 cm^{-1} to the ν(O–H) stretching vibration.[44,45] It is important to notice a decrease in the stretching [Ch][DHP] vibration observed at 1479 cm^{-1} with increasing solvent drying temperature from 25 to 80 °C, and also in the carrageenan absorption bands due to the water molecules enhancing the structural stability by connecting the sulfate groups to the neighbouring hydroxymethyl group.[46]

The absorption band observed at 2164 cm^{-1} for the [Bmim][$C(CN)_3$] sample (Fig. 5b) is attributed to the C–N stretching vibration characteristic of the $[C(CN)_3]^-$ anion.[8,47] For [Bmim][$FeCl_4$]/carrageenan composites, the absorption band at 1163 cm^{-1} is assigned to the aromatic C–H vibrations of the $[Bmim]^+$ cation and the bands at 829 and 1459 cm^{-1} correspond to the aliphatic C–H vibrations of the $[Bmim]^+$ cation.[48,49]

The influence of IL content, type and processing temperature on the mechanical properties of the IL/carrageenan samples are presented in Fig. 5c and d.

Fig. 5c shows that neat carrageenan presents a mechanical behaviour characteristic of a thermoplastic polymer,[50] characterized by an elastic region, corresponding to elastic deformation. Upon the incorporation of [Ch][DHP] into the carrageenan matrix and using a solvent evaporation temperature of 25 °C, a noticeable plastic deformation is observed, decreasing the films stiffness, this behavior being more noticeable for larger IL contents, indicating a plasticizing effect of ILs. Thus, [Ch][DHP] seems to act as a nucleating agent leading to a crystallinity decrease of the samples[51] and in this sense to a decrease in the maximum tensile strength (σ_y). As shown in Fig. 5c, a decrease in σ_y occurs with the IL content increase being independent of the solvent temperature, displaying that the carrageenan has a σ_y of 45.58 MPa and [Ch][DHP]/carrageenan 40% w/w, a σ_y of 11.56 MPa. Furthermore, a small increase in the elastic region is observed for the samples processed at 80 °C, which may be attributed to the plasticizing effect of the IL. The extension of the plastic deformation region is IL type dependent as observed in Fig. 5d. The more noticeable plastic deformation is observed for the carrageenan samples comprising the cation cholinium ([Ch][$FeCl_4$] and [Ch][DHP]), followed by the samples incorporating the ILs [Bmim][$C(CN)_3$] and [Bmim][$FeCl_4$] as a result of the higher cation size of the methylimidazolium based ILs (see Table 1) when compared to the cholinium cation, the cation/anion-carrageenan interactions being favored for cholinium-based ILs. Attending to values obtained for the Young modulus (E') values, obtained from the linear regime at 2% of maximum elongation in the elastic region by the tangent method (Table 3), it is observed that the increase in the elastic region is accompanied by a decrease in E', the yield strength also decreasing and increasing the yielding strain.

As shown in Table 3, for the samples obtained at 25 °C, E' decreases from 748 MPa for neat carrageenan to 145 MPa for the [Ch][DHP]/carrageenan sample with an IL content of 40% w/w. This decrease is IL content dependent, with the E' decreasing with increasing IL content. Furthermore, the mechanical properties are also drying temperature dependent, with E' decreasing from 145 MPa (at 25 °C) to 91 MPa (80 °C) for the [Ch][DHP]/carrageenan sample with 40% w/w IL content because of the higher chain mobility as a result of the temperature increase. The type of IL also influences the mechanical properties of the hybrid samples: smaller choline anions lead to a higher decrease of E' with respect to the neat polymer. Thus, E' decreases in the following order, [Ch][DHP], 91 MPa < [Ch][$FeCl_4$], 261 MPa indicating that polymer-anion interactions are predominant in the determination of the mechanical properties. This behavior is not so prominent for the carrageenan comprising the imidazolium based ILs in which

Table 3 Young modulus and glass transition temperature of the different IL/carrageenan composites

IL/carrageenan	% w/w IL	Solvent evaporation temperature (°C)	$E' \pm 15$ MPa	$T_g \pm 2$ (°C)
[Ch][DHP]	0	25	748	105
	10		667	104
	20		673	104
	40		145	106
	40	80	91	100
[Ch][$FeCl_4$]	40		261	97
[Bmim][$FeCl_4$]	40		207	96
[Bmim][$C(CN)_3$]	40		210	100

no significant differences are observed, with [Bmim][$FeCl_4$]/carrageenan presenting an E' of 207 MPa and [Bmim][$C(CN)_3$]/carrageenan an E' of 210 MPa.

Thermal properties

The influence of IL content and type and solvent evaporation temperature on the thermal characteristics of the IL/carrageenan samples was evaluated by DSC and TGA measurements (Fig. 6).

Fig. 6a and b show the DSC curves for all [Ch][DHP]/carrageenan samples comprising different IL contents obtained at a solvent evaporation of 25 and 80 °C, and for IL/carrageenan samples comprising different ILs obtained at a solvent evaporation temperature of 80 °C, respectively. Independently of the IL content and drying temperature, neat and [Ch][DHP]/carrageenan samples display a single endothermic peak between 60 and 140 °C attributed to the sol–gel transition temperature (T_g).[52] This endothermic peak also occurs in the same range for the hybrid materials, indicating no influence of the IL's type or content on this peak of carrageenan (Table 3). On the other hand, for a given IL content but varying drying temperature, a decrease in this peak is observed when solvent evaporation takes place at 80 °C. This fact is attributed to the transformation of carrageenan molecules from random coils to a double helix structure.[39]

The thermal stability of the IL/carrageenan samples was evaluated by TGA measurements, as presented in Fig. 6c and d. For neat carrageenan, three main weight loss steps are observed. The first stage occurs between 25 and 100 °C and is associated with the adsorbed and bound water loss of the samples.[53] The second degradation step is observed in the range 210 to 330 °C and is attributed to the polymeric backbone $-OSO_3^-$ decomposition.[54] The third and last stage is observed at ~600 °C and corresponds to the decomposition of the carrageenan.[55] Attending to [Ch][DHP]/carrageenan samples (Fig. 6c), it is observed that, independently of the IL content and solvent evaporation temperature, all samples display the same three degradation steps with no significant changes in the decomposition temperatures. However, a decrease in the weight loss occurs when compared to neat carrageenan probably as a result of the IL–carrageenan interactions. The influence of the IL anion type was also evaluated for the samples obtained at a solvent drying temperature of 80 °C (Fig. 6d), the same three degradations being observed. However, for the imidazolium-based carrageenan films, the onset temperature (T_{onset}, calculated from the partial peak resulting from the decomposition of the films), of each individual degradation stage decreases, indicating a decrease in the thermal stability of the films indicating that the higher size of $[Bmim]^+$ cations promotes weaker IL–polymer interactions, resulting in a thermal stability decrease.

Ionic conductivity

The ionic conductivity is an essential parameter determining actuator performance. The ionic conductivity of the developed materials, comprising the different ILs and obtained at room temperature and 80 °C, was obtained from the Nyquist plots obtained in the temperature range from 25 °C to 70 °C (Fig. S1 – ESI†). Regardless of the composite, the Nyquist plot shows three different regions: a semi-circle located in the high frequency range that corresponds to a charge transfer process, a straight line at lower frequencies, characteristic of a charge diffusion process, and finally, the transition between these two phenomena.[56] It is only shown the results of the Arrhenius plots for the ionic conductivity of the IL/carrageenan composites because for neat carrageenan, the ionic conductivity is very low in comparison to the composites (Fig. 7a). Regardless the composite type, increasing the temperature leads to an increase in the ion diffusion caused by an increase in the charge transfer process. The ionic conductivity was calculated from eqn (1) and the typical Arrhenius plots for the different IL/carrageenan composites are shown in Fig. 7.

Fig. 7a shows the ionic conductivity values of the carrageenan and [Ch][DHP]/carrageenan composites with different IL contents (10, 20 and 40% w/w) in the temperature range from

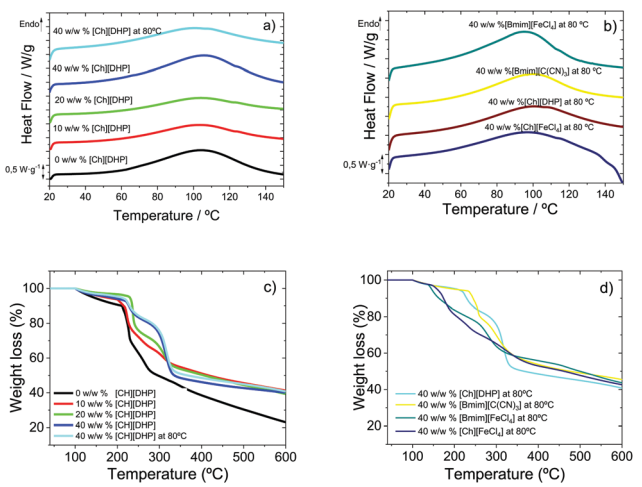

Fig. 6 (a and b) DSC and (c and d) TGA thermograms for: [Ch][DHP]/carrageenan samples containing different IL contents (10, 20 and 40% w/w) and obtained at different drying temperatures (25 and 80 °C) and for IL/carrageenan samples comprising different ILs obtained at a solvent evaporation temperature of 80 °C, respectively.

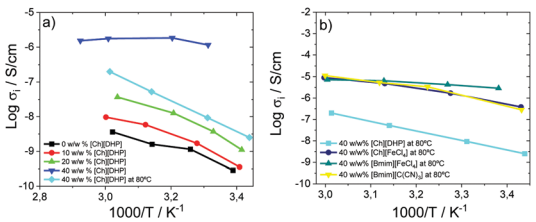

Fig. 7 Arrhenius plots for the ionic conductivity of the IL/carrageenan composites: (a) [Ch][DHP]/carrageenan samples containing different IL contents (10, 20 and 40% w/w) and obtained at different drying temperatures (25 and 80 °C) and (b) IL/carrageenan samples comprising different ILs obtained at a solvent evaporation temperature of 80 °C.

25 °C to 70 °C. Regardless of the IL content, the ionic conductivity increases with the IL incorporation into the carrageenan matrix and with increasing temperature due to improvement of the segmental motion of the polymer chains and of the ionic mobility.[57] It is also observed that the IL content and solvent evaporation temperature affects ionic conductivity, increasing the conductivity with IL content increase due to the larger ionic charge content. At room temperature, the highest ionic conductivity is 1.2×10^{-6} S cm^{-1} for [Ch][DHP] with 40% w/w prepared at 25 °C, probably attributed to the presence of intrinsic water.

Fig. 7b shows the ionic conductivities of 40% w/w IL/carrageenan composites in the same temperature range but obtained after processing at 80 °C. All 40% w/w IL composites show a similar ionic conductivity, independently of the anion type, except for the composite with 40% w/w [Ch][DHP] which shows a lower ionic conductivity as a result of the lowest ionic conductivity of this IL type (<0.4 mS cm^{-1}).

Thus, the ionic conductivity is mainly affected by IL content, due to increases in the carrier concentration inside the composites, but also the solvent evaporation temperature, as it affects the carrageenan final conformation correlated with the double helix conformation.[46]

Electromechanical functional response

Due to their ionic properties as a result of the presence of cations and anions in the polymer matrix, the potential of the developed materials to be applied as actuators was accessed through electromechanical measurements. The results presented in Fig. 8 correspond to the [Ch][DHP]/carrageenan samples comprising different 10, 20 and 40% w/w IL contents, obtained at different solvent drying temperatures (25 and 80 °C) as no bending displacement was observed for the other IL/carrageenan samples comprising [Ch][$FeCl_4$], [Bmim][$FeCl_4$] and [Bmim][$C(CN)_3$] indicating that the carrageenan matrix favours ion diffusion and mobility as a result of the high ion–dipole interactions between the [Ch][DHP] with the carrageenan polymer chain, namely the negatively charged SO_3^- groups of carrageenan with the $[Ch]^+$ cations from the IL. For the samples comprising the imidazolium cation $[Bmim]^+$ the absence of a bending response results, as above-mentioned, from the lower IL–carrageenan interactions in these types of composites as a result of the cation size.

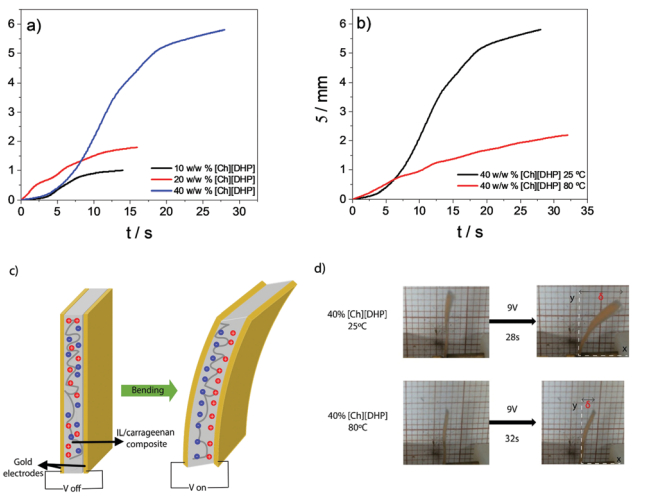

Fig. 8 (a) Displacement of the [Ch][DHP]/carrageenan composites containing 10, 20 and 40% w/w of IL at the same maximum applied voltage (9 V) under a DC field. (b) Bending motion as a function of time for 40% w/w [Ch][DHP]/carrageenan films prepared at solvent evaporation temperatures of 25 °C and 80 °C for an applied voltage of 9 V. (c) Schematic representation of the bending actuation mechanism and (d) optical pictures of the [Ch][DHP]/carrageenan films prepared at solvent evaporation temperatures of 25 °C and 80 °C for an applied voltage of 9 V.

Fig. 8a shows the displacement developed by the sample obtained at 25 °C comprising 10, 20 and 40% w/w of [Ch][DHP] and at 80 °C (Fig. 8b) at an applied voltage of 9 V in DC mode as a function of time. The observed bending response with the applied voltage results from the different sizes of cations and anions and their movement and diffusion to the negative and positive electrode layers, respectively[8,58] (Fig. 8c). As a result, the cations and anions from the IL migrate and redistribute near to the electrodes, leading to a electromechanical response.[58] The maximum displacement was developed by the sample [Ch][DHP]/carrageenan comprising 40% w/w of IL with a maximum displacement of 5.8 mm upon an applied voltage of 9 V (see the ESI,† video S1), followed by 20% w/w of [Ch][DHP] (1.65 mm) and 10% w/w of [Ch][DHP] (0.95 mm). These results are explained from the lower Young modulus obtained for [Ch][DHP]/carrageenan comprising 40% w/w, compared to the other [Ch][DHP]/carrageenan comprising 10 and 20% w/w, and in this sense in a higher ion density, resulting in a higher bending response.

The sample processing temperature also influences the bending motion response. As shown in Fig. 8b and d through the representative images of the bending motion as a function of time for 40% w/w [Ch][DHP]/carrageenan films for an applied voltage of 9 V at solvent evaporation temperatures of 25 °C and 80 °C, the maximum displacement is obtained for the sample 40% w/w of [Ch][DHP]/carrageenan obtained at 25 °C due to the double helix conformation resulting from the interaction between water and the carrageenan chains. Furthermore, the higher bending motion is also attributed to the higher ionic conductivity of this composite (1.2×10^{-6} S cm^{-1}), which can also be related to the presence of water, as identified by TGA curves, the water also acting as a plasticizer, lowering the Young modulus of this sample. In fact, the displacement is governed by the electrical properties of the samples but also by their mechanical properties. For a solvent evaporation temperature of 25 °C, the sample containing 40% w/w of [Ch][DHP] shows the lowest E' (145 MPa), when compared to the samples comprising 10 and 20% w/w of IL, favouring the bending response as a result of ion accumulation. On the other hand, this sample shows a displacement of 2 mm when the solvent evaporation occurs at 80 °C.

The obtained results demonstrate that [Ch][DHP]/carrageen-based materials are suitable to be applied as soft bending actuators.

Conclusions

In the present work, novel naturally derived materials based on iota-carrageenan and different ammonium and imidazolium based ionic liquids (ILs) were developed for actuator applications. [Ch][DHP]/carrageenan samples comprising different [Ch][DHP] contents (10, 20 and 40% w/w) and [Ch][$FeCl_4$], [Bmim][$FeCl_4$] and [Bmim][$C(CN)_3$]/carrageenan samples incorporating 40% w/w of IL were developed.

A non-porous structure was obtained for all samples, being independent of the IL content, type, and solvent evaporation temperature. Increasing the [Ch][DHP] content up to 40% w/w leads to a more compact structure, indicating that, independently of the [Ch][DHP] concentration, the IL is embedded into the carrageenan matrix. Similar results were observed for the other IL/carrageenan samples comprising different ILs. The mechanical properties evaluated from tensile measurements revealed a plasticizing effect as a result of the IL incorporation into the carrageenan matrix, resulting in a decrease of the Young modulus for all the produced composites with respect to the neat polymer. This reduction is IL content dependent, a decrease from 748 MPa for carrageenan to 145 MPa for the sample with 40% w/w of [Ch][DHP] being observed. On the other hand, no significant difference is observed in the thermal stability of the samples.

The ionic conductivity depends on IL content and solvent evaporation temperature, but it is nearly independent of IL type. For [Ch][DHP]/carrageenan composites, the highest ionic conductivity at room temperature is 1.2×10^{-6} S cm^{-1} observed for an IL content 40% w/w processed at 25 °C.

The successful performance of the materials as electromechanical actuators was demonstrated, the maximum electromechanical bending displacement (5.8 mm upon an applied voltage of 9 V) being obtained by the [Ch][DHP]/carrageenan sample containing 40% w/w of IL and processed at 25 °C. The obtained results demonstrate the suitability of the developed natural-based bending actuator for environmentally friendlier soft robotic applications, among others. Additionally, due to the biocompatibility of choline-based ILs, [Ch][DHP]/carrageenan samples can also be evaluated as soft actuators or active scaffolds in biomedical applications.

Author contributions

João P. Serra: methodology; validation; formal analysis; investigation; writing – original draft; writing – review & editing. Liliana C. Fernandes: methodology; validation; formal analysis; investigation; writing – original draft; writing -review & editing. Daniela M. Correia: conceptualization; methodology; validation; formal analysis; investigation; writing – original draft; writing – review & editing. Carmen R. Tubio: investigation; validation; methodology; writing – original draft; writing – review & editing. J. L. Vilas-Vilela: validation; formal analysis; investigation; writing – original draft; writing – review & editing. Mohammad Tariq: validation; formal analysis; investigation; writing – original draft; writing – review & editing. José M. M. S. S. Esperança: validation; formal analysis; investigation; writing – original draft; writing – review & editing. Carlos M. Costa: conceptualization; methodology; validation; formal analysis; investigation; writing – original draft; writing – review & editing. Senentxu Lanceros-Mendez: conceptualization; methodology; resources; funding acquisition; validation; project administration; writing – original draft; writing – review & editing.

Conflicts of interest

There are no conflicts to declare.

Acknowledgements

This work was supported by the Portuguese Foundation for Science and Technology (FCT) under strategic funding UID/FIS/04650/2020, UID/QUI/0686/2020, UIDB/50006/2020, UIDP/50006/2020 and LA/P/0008/2020, project PTDC/FIS-MAC/28157/2017, and grants SFRH/BD/145345/2019 (L. C. F.), SFRH/BPD/121526/2016 (D. M. C.), 2021.08158.BD (J. S.) and Investigator FCT Contract 2020.04028.CEECIND (C. M. C.). The authors acknowledge funding by the Spanish State Research Agency (AEI) and the European Regional Development Fund (ERFD) through the project PID2019-106099RB-C43/AEI/10.13039/501100011033. The authors also acknowledge funding from the Basque Government Industry Department under the ELKARTEKprogram. Technical and human support provided by SGIker (UPV/EHU, MICINN, GV/EJ, EGEF and ESF) is gratefully acknowledged.

References

1 R. Bogue, *Assembly Automation*, 2014.
2 X. Zhang, Q. Lu, C. Yang, S. Zhao, Y. Chen, H. Niu, P. Zhao and W. Wang, *Eur. Polym. J.*, 2019, **112**, 291–300.
3 M. Giaquinto, *Results Opt.*, 2021, **2**, 100051.
4 C. Ribeiro, V. Sencadas, D. M. Correia and S. Lanceros-Méndez, *Colloids Surf., B*, 2015, **136**, 46–55.
5 H. Salazar, J. Nunes-Pereira, D. Correia, V. Cardoso, R. Gonçalves, P. Martins, S. Ferdov, M. Martins, G. Botelho and S. Lanceros-Méndez, *Mater. Chem. Phys.*, 2016, **183**, 430–438.
6 H. Lee, M. Yanilmaz, O. Toprakci, K. Fu and X. Zhang, *Energy Environ. Sci.*, 2014, **7**, 3857–3886.
7 J. Oliveira, V. Correia, H. Castro, P. Martins and S. Lanceros-Mendez, *Addit. Manuf.*, 2018, **21**, 269–283.
8 D. Correia, L. Fernandes, N. Pereira, J. Barbosa, J. Serra, R. Pinto, C. Costa and S. Lanceros-Méndez, *Appl. Mater. Today*, 2021, **22**, 100928.
9 S. J. Rupitsch, *Piezoelectric sensors and actuators*, Springer, 2019.
10 P. Martins, D. Correia, V. Correia and S. Lanceros-Mendez, *Phys. Chem. Chem. Phys.*, 2020, **22**, 15163–15182.
11 D. M. Correia, L. C. Fernandes, P. M. Martins, C. García-Astrain, C. M. Costa, J. Reguera and S. Lanceros-Méndez, *Adv. Funct. Mater.*, 2020, **30**, 1909736.

12 A. Paiva, R. Craveiro, I. Aroso, M. Martins, R. L. Reis and A. R. C. Duarte, *ACS Sustainable Chem. Eng.*, 2014, **2**, 1063–1071.
13 Z. Lei, B. Chen, Y.-M. Koo and D. R. MacFarlane, *Chem. Rev.*, 2017, **117**, 6633–6635.
14 J. C. Barbosa, J. P. Dias, S. Lanceros-Méndez and C. M. Costa, *Membranes*, 2018, **8**, 45.
15 Z. Xue, D. He and X. Xie, *J. Mater. Chem. A*, 2015, **3**, 19218–19253.
16 D. Correia, C. Ribeiro, G. Botelho, J. Borges, C. Lopes, F. Vaz, S. Carabineiro, A. Machado and S. Lanceros-Méndez, *Appl. Surf. Sci.*, 2016, **371**, 74–82.
17 H. Bar, R. Ikan and Z. Aizenshtat, *J. Anal. Appl. Pyrolysis*, 1988, **14**, 73–79.
18 P. Worsfold, A. Townshend, C. F. Poole and M. Miró, *Encyclopedia of analytical science*, Elsevier, 2019.
19 C. M. Costa, M. T. Machiavello, J. G. Ribelles and S. Lanceros-Méndez, *J. Mater. Sci.*, 2013, **48**, 3494–3504.
20 E. Hysa, A. Kruja, N. U. Rehman and R. Laurenti, *Sustainability*, 2020, **12**, 4831.
21 C. Harper and M. Snowden, *Environment and society: Human perspectives on environmental issues*, Taylor & Francis, 2017.
22 OECD, 2019.
23 A. Rudin and P. Choi, *The elements of polymer science and engineering*, Academic Press, 2012.
24 O. Olatunji, *Natural polymers: industry techniques and applications*, Springer, 2015.
25 M. Mangione, D. Giacomazza, D. Bulone, V. Martorana, G. Cavallaro and P. San, Biagio, *Biophys. Chem.*, 2005, **113**, 129–135.
26 C.-H. Tang, H. Wu, Z. Chen and X.-Q. Yang, *Food Res. Int.*, 2006, **39**, 87–97.
27 A. B. A. Ahmed, M. Adel, P. Karimi and M. Peidayesh, in *Advances in Food and Nutrition Research*, ed. S.-K. Kim, Academic Press, 2014, vol. 73, pp. 197–220.
28 A. Bartkowiak and D. Hunkeler, *Colloids Surf., B*, 2001, **21**, 285–298.
29 M. Khotimchenko, V. Tiasto, A. Kalitnik, M. Begun, R. Khotimchenko, E. Leonteva, I. Bryukhovetskiy and Y. Khotimchenko, *Carbohydr. Polym.*, 2020, 116568.
30 L. C. Geonzon, F. B. A. Descallar, L. Du, R. G. Bacabac and S. Matsukawa, *Food Hydrocolloids*, 2020, 106039.
31 K. M. Zia, S. Tabasum, M. Nasif, N. Sultan, N. Aslam, A. Noreen and M. Zuber, *Int. J. Biol. Macromol.*, 2017, **96**, 282–301.
32 F. Soleimani, M. Sadeghi and H. Shahsavari, *Indian J. Sci. Technol.*, 2012, **5**, 2143–2147.
33 T. Jayaramudu, G. M. Raghavendra, K. Varaprasad, R. Sadiku, K. Ramam and K. M. Raju, *Carbohydr. Polym.*, 2013, **95**, 188–194.
34 M.-K. Kim and J.-S. Lee, *ACS Nano*, 2018, **12**, 1680–1687.
35 P. Martins, D. M. Correia, V. Correia and S. Lanceros-Mendez, *Phys. Chem. Chem. Phys.*, 2020, **22**, 15163–15182.
36 S. Matchawet, A. Kaesaman, N. Vennemann, C. Kumerlöwe and C. Nakason, *Eur. Polym. J.*, 2017, **87**, 344–359.
37 L. Migliorini, T. Santaniello, S. Rondinini, P. Saettone, M. Comes Franchini, C. Lenardi and P. Milani, *Sens. Actuators, B*, 2019, **286**, 230–236.
38 D. M. Correia, E. Lizundia, R. M. Meira, M. Rincón-Iglesias and S. Lanceros-Méndez, *Materials*, 2020, **13**, 2294.
39 N. Tanusorn, N. Thummarungsan, W. Sangwan, W. Lerdwijitjarud and A. Sirivat, *Int. J. Biol. Macromol.*, 2018, **118**, 2098–2107.
40 Z. Chongmin, S. Takehiko, J.-K. Akiko, F. Emiko, K. Akiko, T. Mizuki and I. Yasuhiro, *Bull. Chem. Soc. Jpn.*, 2007, **80**, 2365–2374.
41 N. A. A. Ghani, F. H. Anuar, A. Ahmad, N. N. Mobarak, I. J. Shamsudin, M. Z. Dzulkipli and N. H. Hassan, *Sains Malays.*, 2020, **49**, 305–313.
42 L. Pereira, A. M. Amado, A. T. Critchley, F. Van de Velde and P. J. Ribeiro-Claro, *Food Hydrocolloids*, 2009, **23**, 1903–1909.
43 N. G. Rajasulochana, *Asian J. Chem.*, 2009, **21**, 4547–4552.
44 C. Du, B. Zhao, X.-B. Chen, N. Birbilis and H. Yang, *Sci. Rep.*, 2016, **6**, 1–14.
45 R. Meira, D. M. Correia, S. Ribeiro, P. Costa, A. C. Gomes, F. Gama, S. Lanceros-Méndez and C. Ribeiro, *ACS Appl. Polym. Mater.*, 2019, **1**, 2649–2658.
46 N. A. A. Ghani, R. Othaman, A. Ahmad, F. H. Anuar and N. H. Hassan, *Arabian J. Chem.*, 2019, **12**, 370–376.
47 C. Y. Peñalber, Z. Grenoble, G. A. Baker and S. Baldelli, *Phys. Chem. Chem. Phys.*, 2012, **14**, 5122–5131.
48 Z.-L. Xie, A. Jeličić, F.-P. Wang, P. Rabu, A. Friedrich, S. Beuermann and A. Taubert, *J. Mater. Chem.*, 2010, **20**, 9543–9549.
49 D. Correia, L. Fernandes, C. García-Astrain, M. Tariq, J. M. S. S. Esperança, V. de Zea Bermudez and S. Lanceros-Méndez, *Composites, Part B*, 2019, **178**, 107516.
50 C. M. Costa, V. Sencadas, I. Pelicano, F. Martins, J. G. Rocha and S. Lanceros-Méndez, *J. Non-Cryst. Solids*, 2008, **354**, 3871–3876.
51 R. M. Meira, D. M. Correia, S. Ribeiro, P. Costa, A. C. Gomes, F. M. Gama, S. Lanceros-Méndez and C. Ribeiro, *ACS Appl. Polym. Mater.*, 2019, **1**, 2649–2658.
52 M. Alnaief, R. Obaidat and H. Mashaqbeh, *Carbohydr. Polym.*, 2018, **180**, 264–275.
53 M. Sadeghi, *Braz. J. Chem. Eng.*, 2012, **29**, 295–305.
54 F. N. Jumaah, N. N. Mobarak, A. Ahmad, M. A. Ghani and M. Y. A. Rahman, *Ionics*, 2015, **21**, 1311–1320.
55 S. Ma, L. Chen, X. Liu, D. Li, N. Ye and L. Wang, *Int. J. Green Energy*, 2012, **9**, 13–21.
56 B.-Y. Chang and S.-M. Park, *Annu. Rev. Anal. Chem.*, 2010, **3**, 207–229.
57 R. Leones, C. Costa, A. Machado, J. M. S. S. Esperança, M. M. Silva and S. Lanceros-Méndez, *Electroanalysis*, 2015, **27**, 457–464.
58 D. M. Correia, J. C. Barbosa, C. M. Costa, P. M. Reis, J. M. S. S. Esperança, V. de Zea Bermudez and S. Lanceros-Méndez, *J. Phys. Chem. C*, 2019, **123**, 12744–12752.